

Organic Fouling and Chemical Cleaning of Nanofiltration Membranes: Measurements and Mechanisms

QILIN LI*[†] AND
MENACHEM ELIMELECH[‡]

Department of Civil, Construction, and Environmental Engineering, Oregon State University, Corvallis, Oregon 97331, and Department of Chemical Engineering, Environmental Engineering Program, Yale University, New Haven, Connecticut 06520-8286

Fouling and subsequent chemical cleaning of nanofiltration (NF) membranes used in water quality control applications are often inevitable. To unravel the mechanisms of organic fouling and chemical cleaning, it is critical to understand the foulant–membrane, foulant–foulant, and foulant–cleaning agent interactions at the molecular level. In this study, the adhesion forces between the foulant and the membrane surface and between the bulk foulant and the fouling layer were determined by atomic force microscopy (AFM). A carboxylate modified AFM colloid probe was used as a surrogate for humic acid, the major organic foulant in natural waters. The interfacial force data were combined with the NF membrane water flux measurements to elucidate the mechanisms of organic fouling and chemical cleaning. A remarkable correlation was obtained between the measured adhesion forces and the fouling and cleaning behavior of the membrane under various solution chemistries. The AFM measurements further confirmed that divalent calcium ions greatly enhance natural organic matter fouling by complexation and subsequent formation of intermolecular bridges among organic foulant molecules. Efficient chemical cleaning was achieved only when the calcium ion bridging was eliminated as a result of the interaction between the chemical cleaning agent and the fouling layer. The cleaning efficiency was highly dependent on solution pH and the concentration of the chemical cleaning agent.

Introduction

Nanofiltration (NF) membranes are used in a wide range of drinking water, wastewater, and industrial applications (1, 2). A major obstacle for the efficient application of NF membrane technology is the phenomenon of membrane fouling. Fouling results in deterioration of membrane performance (i.e., permeate water flux and quality) and ultimately shortens membrane life. Among the potential foulants that are ubiquitous in natural and waste waters, dissolved organic matter is the most recalcitrant. Therefore, understanding the causes of membrane fouling and devel-

oping strategies for fouling control and membrane cleaning are major challenges.

Membrane fouling is determined by the coupled influence of physical and chemical interactions (3–5). These interactions and the resulting properties of the fouling layer are controlled by the foulant characteristics, feedwater solution chemistry (pH, ionic strength, divalent cation concentration), membrane properties (surface charge, hydrophobicity, roughness), and hydrodynamic conditions (permeate flux, cross-flow velocity). The physicochemical characteristics of the foulant, such as charge and molecular conformation, directly control the rate of foulant accumulation and the properties of the fouling layer and, therefore, have significant impact on membrane permeate flux (6, 7). For natural organic matter (NOM), solution chemistry also controls the charge and conformation of NOM macromolecules and, thus, the structure and hydraulic resistance of the foulant deposit layer (3, 8–12). Divalent cations, such as Ca^{2+} , may react with organic molecules to form metal–NOM complexes, resulting in a highly compacted fouling layer and substantial flux decline (3, 5, 10, 11, 13–17).

Despite the vast efforts to reduce membrane fouling, for instance, by improving membrane properties, optimizing operational conditions, and pretreatment of feedwater, fouling is still inevitable. Indeed, several pretreatment processes designed to solve specific fouling problems may lead to other problems (18). As a result, chemical cleaning is a necessary process to ensure sustainable operation of membrane systems (19–24). Membrane cleaning is often applied when a significant decrease in permeate flux or salt rejection is observed or when the transmembrane pressure has to be raised significantly to maintain the designed water flux (25).

For chemical cleaning of fouled membranes, five categories of cleaning agents are commonly used: alkalines, acids, metal chelating agents, surfactants, and enzymes (21, 26). Commercial cleaning products are usually mixtures of these compounds, but the actual composition is often unknown. Consequently, all chemical cleaning studies conducted so far were not able to provide useful information to elucidate the mechanisms of chemical cleaning.

Chemical cleaning of fouled membranes is realized through chemical reactions between the chemical agents and the foulants. A cleaning agent cleans the membrane by removing the foulants, changing the morphology of the foulants, or altering the surface chemistry of the fouling layer (27–29). Consequently, proper selection of chemical cleaning agents relies on our mechanistic understanding of the foulant–particularly the chemical reactions between the foulant and the cleaning chemicals. To date, mechanistic studies on chemical cleaning of polymeric membranes are rather scarce. Most reported work utilized commercial membrane cleaning products, and the cleaning procedures followed were specified by the membrane manufacturers (27, 30–32).

The effectiveness of chemical cleaning was found to depend on various factors, including temperature, pH, concentration of the cleaning chemicals, contact time with the cleaning solution, and operating conditions, such as cross-flow velocity and pressure (21, 33–35). However, the test conditions used in these studies were very specific in terms of raw water quality, membrane properties, and operating conditions. The results obtained from such studies often disagree and are therefore not applicable for other situations. This further points out to the need for more controlled and

* Corresponding author phone: (541)737-9910; fax: (541)737-3099; e-mail: qilin.li@oregonstate.edu.

[†] Oregon State University.

[‡] Yale University.

fundamental studies on chemical cleaning of NF (and other) membranes.

Atomic force microscopy (AFM) has been used to measure various forces in aqueous solutions, including electrostatic, van der Waals, adhesion, steric, bridging, depletion, hydration, and hydrophobic interactions (36–49). It is not until very recently that AFM force measurements have been applied to membrane research (50–54). Measurement of interaction forces between a colloid probe and a membrane surface allows quantification of the electrostatic double layer interactions when the colloid probe approaches the membrane surface, and of the adhesion force when the colloid probe is withdrawn after it has been in contact with the membrane surface. Quantification of such interactions can provide useful information pertaining to membrane fouling mechanisms and, consequently, the mechanisms of membrane chemical cleaning. However, to date, no work has been done to establish direct correlation between the measured forces and the membrane fouling behavior. Moreover, the effect of chemical cleaning agents on foulant interactions and adhesion has never been studied before. Quantification of the interaction forces involved in fouling and chemical cleaning of fouled membranes is a key to the development of a mechanistic description of the processes involved.

In this study, atomic force microscopy was used to quantify the interaction forces between the foulant and the clean or fouled membrane surface. To better understand the role of solution chemistry, the force measurements and the bench-scale fouling/chemical cleaning experiments were performed under various solution conditions—total ionic strength, divalent cation concentration, and pH—relevant to NOM membrane fouling and chemical cleaning. Measured interfacial forces correlated directly with the membrane fouling rate and chemical cleaning performance and, thus, provide molecular level information to elucidate the mechanisms of membrane organic fouling and chemical cleaning.

Materials and Methods

NF Membrane. A thin-film composite NF membrane, denoted NF-270 by the manufacturer, was used (FilmTec Corp., Minneapolis, MN). It is a semiaromatic, piperazine based polyamide membrane (55). Membrane samples for the fouling/chemical cleaning experiments were stored in deionized water at 5 °C, with water replaced regularly. For interfacial force measurements, membrane samples were stored dry. All membrane samples were rinsed thoroughly with deionized water prior to use.

Model Foulant. The model organic foulant used was Suwannee River humic acid (SRHA) standard (International Humic Substances Society, St. Paul, MN). SRHA was obtained in a freeze-dried form. Stock solution (1 g/L) was prepared by dissolving the freeze-dried SRHA in deionized water and adjusting the pH to 8.2 through the addition of NaOH. Mixing was provided until complete dissolution of the SRHA. The stock solution was then stored in a sterilized glass bottle at 5 °C.

Chemical Cleaning Solutions. The model chemical cleaning solutions tested were deionized water as a baseline; NaOH (pH 11) as an alkaline solution; certified grade sodium ethylenediaminetetraacetate, EDTA, as a metal chelating agent; and certified grade sodium dodecyl sulfate, SDS, as an anionic surfactant. The NaOH, EDTA, and SDS were purchased from Fisher Scientific (Pittsburgh, PA). These chemical agents are common ingredients in commercial chemical cleaning solutions for organic-fouled membranes (26). Solutions were freshly prepared with deionized water right before the experiment.

Solution Chemistry. Bench-scale membrane fouling/chemical cleaning experiments and interfacial force measurements were conducted at a total ionic strength ranging

from 10 to 100 mM and with various ionic compositions. Feed solution pH was kept at 8.1 in all experiments by adding 1 mM NaHCO₃ and a small amount of NaOH. In some experiments, certified grade CaCl₂ or MgCl₂ (Fisher Scientific, Pittsburgh, PA) was added at a concentration of 1 mM to study the effect of divalent cations on fouling and chemical cleaning. The desired total ionic strength was obtained by adjusting the concentration of NaCl (Fisher Scientific, Pittsburgh, PA). In all experiments, the SRHA concentration was fixed at 20 mg/L. The SRHA concentration was confirmed by measuring total organic carbon (TOC) of the feed solution with a TOC analyzer (Shimadzu Corporation, Kyoto, Japan) and comparing the measured value with the organic carbon content provided by the International Humic Substances Society. Chemical cleaning experiments with EDTA or SDS were conducted at ambient (unadjusted) pH or at pH 11 by adding NaOH to the cleaning solution. The EDTA concentration used was 1 mM while SDS concentrations tested were 1, 5, 10, and 35 mM.

NF Membrane Characterization. Membrane surface roughness was determined by surface imaging using a Multimode atomic force microscope (AFM) (Digital Instruments, Santa Barbara, CA). Imaging was performed in tapping mode in deionized water in a fluid cell using an oxide sharpened SiN probe (Veeco Metrology Group, Santa Barbara, CA). Results show that the NF-270 membrane is relatively smooth, as expected for piperazine based thin-film composite membranes (55). The zeta potential was determined from streaming potential measurements using an electrokinetic analyzer (BI-EKA, Brookhaven Instruments Corp., Holtsville, NY) (56, 57). Measurements were conducted under solution chemical conditions similar to those used in the bench-scale fouling/chemical cleaning experiments. The membrane was negatively charged under all chemical conditions investigated.

Bench-Scale Fouling and Chemical Cleaning Experiments. Fouling and chemical cleaning experiments were conducted in a bench-scale dead-end filtration system shown schematically in Figure 1. The filtration unit comprises a stainless steel stirred cell, modified from a commercial system (Millipore Corporation, Bedford, MA). The volume of the cell is 400 mL and it houses a 76 mm diameter membrane sample. Two stainless steel reservoirs hold the electrolyte solution and the feed foulant solution, respectively. Pressure, provided by a compressed N₂ tank, can be applied to either of the feed reservoirs or directly to the stirred cell via a five-port valve. Permeate water is collected and the mass is monitored continuously during the experiments by an analytical balance connected to a computer. Permeate flux was calculated from the change in the cumulative mass of permeate water with time.

The fouling and chemical cleaning experimental protocol can be divided into four steps: compacting, conditioning, fouling, and chemical cleaning, as shown schematically in Figure 2. First, the stirred cell was filled with deionized water and the membrane was compacted at 120 psi (827 kPa) until the permeate flux stabilized. In the next stage, an electrolyte solution containing identical electrolyte concentrations to be used in the fouling run was fed to the cell from the corresponding reservoir to condition the membrane and to establish a fouling-free baseline for at least 2 h. During the filtration of the electrolyte solution, the pressure was adjusted to reach the desired initial permeate flux for the fouling run. The initial permeate flux was kept constant in all experiments at $18.0 \pm 2 \mu\text{m/s}$, with the applied pressure used to obtain this flux ranging from 98 to 120 psi. After the membrane was equilibrated with the electrolyte solution and a constant flux was attained, the organic foulant (SRHA) solution in the second reservoir was filtered through the membrane at the same pressure to initiate fouling. Fouling continued until

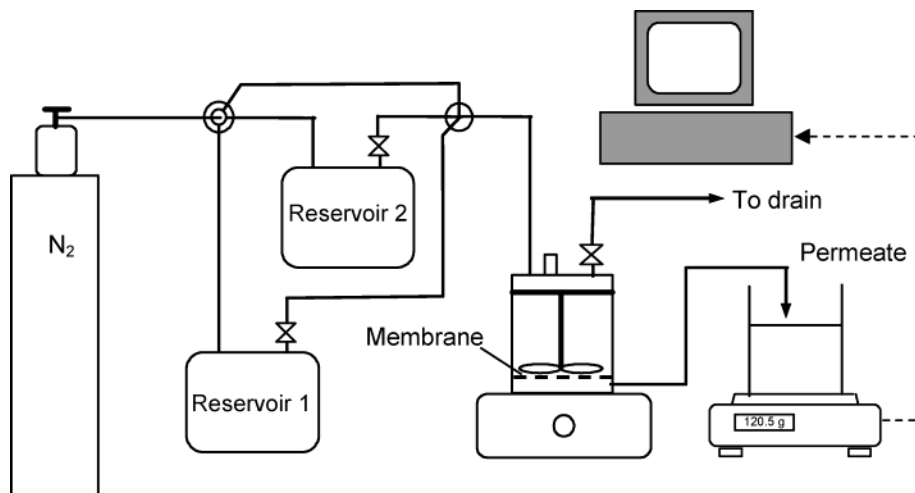


FIGURE 1. Schematic of the membrane filtration system used to study NF membrane fouling and chemical cleaning.

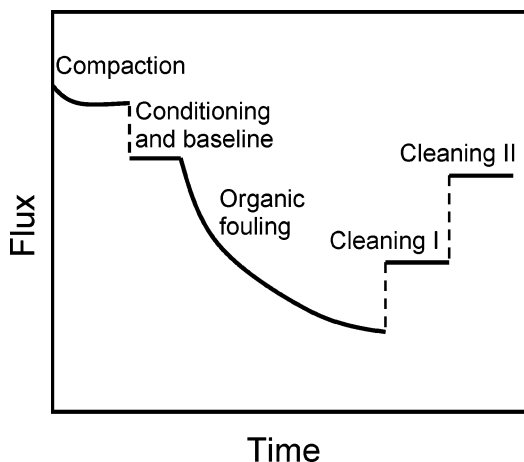


FIGURE 2. Experimental protocol for the fouling/chemical cleaning experiments.

the permeate flux reached a predetermined final flux. During the conditioning and fouling stages, the mixing in the stirred cell was maintained at 225 rpm. Samples were taken from the permeate line at predetermined times and monitored for organic and electrolyte concentrations. Permeate TOC concentration was determined using a TOC analyzer (Shimadzu Corporation, Kyoto, Japan) and cation concentrations were measured by ICP-AES (Perkin-Elmer, Boston, MA). The last step in the experimental protocol was chemical cleaning of the fouled membrane. Cleaning involved the sequential addition of two batches of 250 mL of cleaning solution and mixing at 470 rpm for 10 min for each batch. The filtration unit was rinsed thoroughly with deionized water after each cleaning procedure to remove the residual cleaning solution. Filtration was then resumed with the foulant-free electrolyte solution and the permeate flux was measured to assess the chemical cleaning efficiency. For this step, the applied pressure and mixing rate were identical to those used during the conditioning and fouling stage. In cases where two cleaning solutions are likely to interfere with each other, separate fouling/chemical cleaning experiments were conducted.

Interfacial Force Measurement. AFM was used to measure the interfacial forces between the foulant and the membrane as well as those between the foulant in the bulk solution and the foulant in the fouling layer. The force measurements were performed with a colloid probe, modified from a commercial SiN AFM probe, as described below.

Because carboxylic groups are the predominant functional groups of humic acid, a carboxylate modified latex (CML)

particle (Interfacial Dynamics Corp., Portland, OR) was used as a surrogate for humic acid. The CML particle ($4 \mu\text{m}$ in diameter) contains a somewhat porous, highly charged layer of carboxylate groups, with a titrated surface charge of $139.5 \mu\text{C}/\text{cm}^2$. The colloid probe was made by attaching the CML particle to a tipless SiN probe (Veeco Metrology Group, Santa Barbara, CA). A drop of the CML colloidal suspension was first spread on a freshly cleaved mica surface and dried with filtered ($0.5\text{-}\mu\text{m}$ filter) Ar gas. Using a home-built micro-manipulator, a small amount of Scotch-Weld epoxy adhesive (3M Industrial Adhesive and Tapes, St. Paul, MN) was applied to the free end of the tipless cantilever. A single CML particle was then attached to the cantilever end by the glue, with only a small surface area of the particle being in contact with the glue. After curing, the strength of the colloid probe was tested by applying forces to the attached particle from different angles using another unmodified probe. All force measurements were conducted using the same colloid probe. The probe was carefully examined before and after each use to ensure integrity.

Force measurements were conducted in a fluid cell with a close input/output loop. Solution conditions tested were similar to those used in the bench-scale fouling/chemical cleaning experiments. Before injection of each solution, the cell was rinsed with 6 mL of deionized water and another 6 mL of the test solution. After injection, the membrane was equilibrated with the test solution for at least 30 min before force measurement. Because of possible local membrane surface heterogeneities, force measurements were performed at five different locations on a $1 \mu\text{m} \times 1 \mu\text{m}$ area. At least five measurements were taken at each location.

Both extending (approaching) and retracting force curves were obtained by the AFM. The raw force data were first processed to remove optical interference. The interference-free raw data, that is, cantilever deflection versus cantilever displacement curves, were then converted to force versus surface-to-surface separation curves using the method reported by Ducker et al. (37). Ten force curves were chosen to obtain the average force curve for a given solution condition. The variability in the force data was relatively small, presumably because of the relatively smooth surface of the NF-270 membrane.

Results and Discussion

Overview. Quantification of NOM fouling is essential for understanding chemical cleaning of fouled membranes. Therefore, experimental results of NF membrane organic fouling and relevant AFM force measurements are presented first. This is followed by presentation of chemical cleaning of the NOM fouled NF membranes and the pertaining

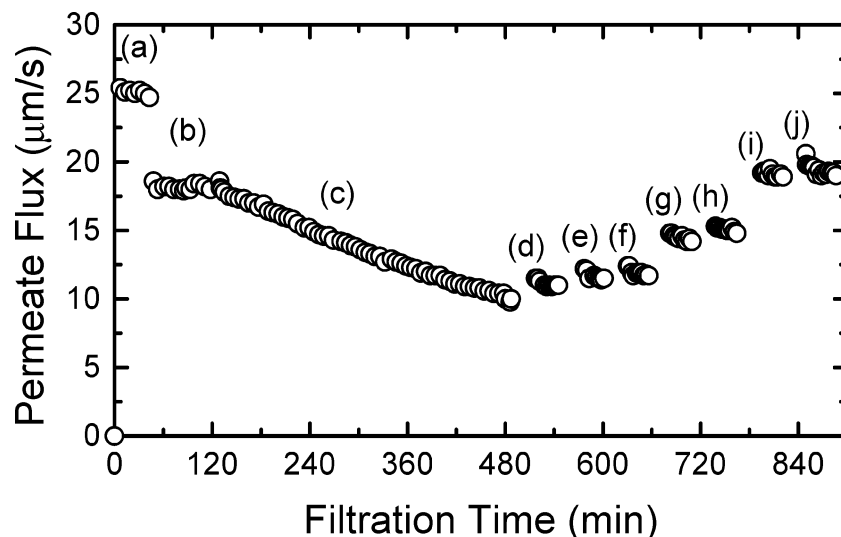


FIGURE 3. Membrane permeate flux at different stages of the fouling/chemical cleaning experiment. (a) Membrane compaction with deionized water; (b) conditioning with electrolyte solution (total ionic strength = 10 mM, Ca^{2+} = 1 mM, pH = 8.1); (c) fouling with SRHA solution (SRHA = 20 mg/L, total ionic strength = 10 mM, Ca^{2+} = 1 mM, pH = 8.1); (d) flux with foulant-free electrolyte solution after cleaning with deionized water; (e) flux with foulant-free electrolyte solution after cleaning with 1 mM SDS at ambient pH; (f) flux with foulant-free electrolyte solution after cleaning with 1 mM SDS at pH 11; (g) flux with foulant-free electrolyte solution after cleaning with 5 mM SDS at ambient pH; (h) flux with foulant-free electrolyte solution after cleaning with 5 mM SDS at pH 11; (i) flux with foulant-free electrolyte solution after cleaning with 10 mM M SDS at ambient pH; and (j) flux of electrolyte solution after cleaning with 10 mM SDS at pH 11.

interfacial force measurements. Last, on the basis of these results, mechanisms of NOM fouling and chemical cleaning are proposed and discussed.

An illustration of permeate flux behavior during an entire run involving membrane compaction, conditioning, fouling, and chemical cleaning is shown in Figure 3. The permeate flux during the membrane conditioning with the electrolyte solution was very stable. This behavior is attributed to the low salt rejection of the NF-270 membrane (44% for Na^+ and 53% for Ca^{2+}), such that flux decline caused by the increased salt concentration and the corresponding increase in osmotic pressure is insignificant. Therefore, the flux decline observed during the fouling stage with the SRHA solution is attributable to accumulation of the organic foulant on the membrane surface. Subsequent chemical cleaning by sequentially increasing the cleaning agent (SDS) concentration or changing the solution pH demonstrates increased recovery of the membrane permeate flux because of the removal of the foulant (NOM) from the membrane surface.

Natural Organic Matter Fouling of the NF Membrane.

Experimental results showing the influence of total ionic strength and divalent cations on organic fouling of the NF-270 membrane are presented below. A detailed description of the mechanisms involved is presented later in this paper following the discussion on the relevant AFM measurements.

(a) Effect of Total Ionic Strength. Fouling experiments were conducted at total ionic strengths of 10 and 100 mM, with Na^+ as the only cation in the feed solution. The two different ionic strengths resulted in essentially the same flux decline rate (Figure 4), indicating insignificant effect of total ionic strength on SRHA fouling of the NF-270 membrane. The fouling rate in both cases was relatively low considering the high concentration of SRHA used (20 mg/L), with only 11% permeate flux decline during the 300-min filtration. These data confirm that charge screening because of increased ionic strength does not play a major role in NOM fouling (3). An ionic strength of 100 mM of an indifferent 1:1 electrolyte was insufficient to cause significant conformational change of SRAH macromolecules to induce significant fouling.

(b) Role of Divalent Cations. Divalent cations have been reported to enhance NOM fouling by forming complexes

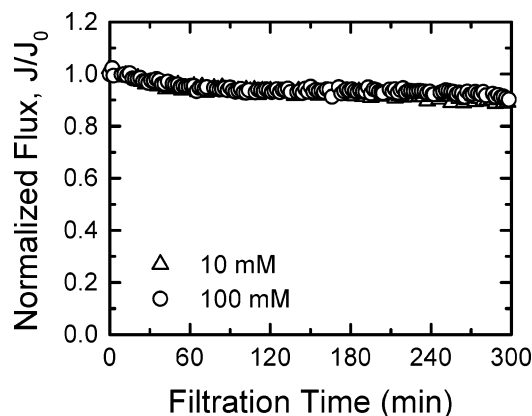


FIGURE 4. Permeate flux decline at different total ionic strengths. The feed solution contained 20 mg/L SRHA, 1 mM NaHCO_3 , and NaCl to adjust the total ionic strength to 10 or 100 mM. Other experimental conditions: initial permeate flux = 1.82×10^{-5} m/s and pH = 8.1.

with NOM and neutralizing negative charges of NOM molecules more effectively than monovalent cations (3, 5, 10, 11, 13–17). Fouling experiments were conducted at a total ionic strength of 10 mM, with 1 mM Ca^{2+} or Mg^{2+} in the feed solution to determine the effect of divalent cations on membrane flux decline. Ca^{2+} and Mg^{2+} were chosen as model divalent cations because they are the major divalent cations in surface waters. As shown in Figure 5, Mg^{2+} slightly increased the membrane flux decline rate compared to Na^+ , whereas Ca^{2+} dramatically enhanced membrane fouling. The membrane permeate flux declined by approximately 11% over a period of 300 min when divalent cations were absent in the feed solution. When Ca^{2+} cations were present, the permeate flux decreased markedly by 49% within 258 min. Surprisingly, however, when Mg^{2+} was present, the flux declined by only 16% over a period of 300 min, slightly higher than with monovalent cations (Na^+) but much less than with Ca^{2+} cations. The dramatic effect of Ca^{2+} on membrane fouling, compared to Na^+ and Mg^{2+} ions, will be discussed later when presenting the corresponding interfacial force measurements.

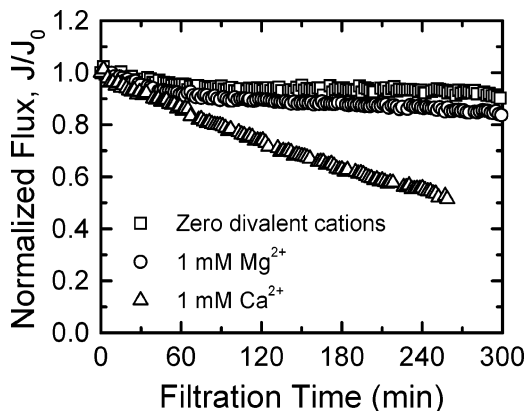


FIGURE 5. Effect of divalent cations on permeate flux decline. The feed solution contained 20 mg/L SRHA, 1 mM NaHCO₃, divalent cations as indicated, and NaCl to adjust the total ionic strength to 10 mM. Other experimental conditions: initial permeate flux = 1.82 × 10⁻⁵ m/s and pH = 8.1.

Interaction Forces between NOM and Clean or Fouled Membrane Surface. Because of the very small pores of NF membranes, surface fouling is the dominant fouling mechanism in nanofiltration. Membrane surface fouling is caused by foulant accumulation (deposition) on the membrane surface. Therefore, the fouling process is controlled by the interactions between the foulant and the clean (at the initial stage of fouling) and fouled membrane surfaces. Interfacial force measurements using an AFM colloid probe can thus provide a quantitative assessment of these interactions.

According to Derjaguin's approximation (58), the interaction force between a sphere and a flat surface is related to the interaction energy per unit area:

$$F(h) = 2\pi RW(h) \quad (1)$$

Here, $F(h)$ is the interaction force between a sphere and a flat surface separated by a distance h , R is the radius of the spherical particle, and $W(h)$ is the interaction energy per unit area between a sphere and a flat surface separated by a distance of h . As shown in eq 1, the interaction energy W is equal to F/R multiplied by a factor of 2π . Moreover, the term F/R normalizes the interaction force F by the radius of the particle R , which allows forces measured with AFM colloid probes of different sizes to be compared. Therefore, all AFM force data will be presented as F/R versus distance.

Similarly, the adhesion force, F_{ad} , normalized by the radius of the particle is proportional to the energy per unit area required to separate the particle and the flat surface by an infinite distance, $W(\infty)$ (58):

$$F_{ad} = 2\pi RW(\infty) \quad (2)$$

Therefore, F_{ad}/R can also be viewed as a measure of the energy required to prevent a foulant from accumulating on the membrane surface. For a given system, F_{ad}/R should be a good indicator of the membrane fouling potential.

During the initial stage of fouling, the membrane surface is clean. Therefore, interaction forces between the foulant and the clean membrane surface (i.e., foulant–membrane interactions) determine the initial fouling rate. After the membrane surface is fouled by the organic foulant, the rate of organic foulant accumulation and, consequently, membrane fouling is determined by the attachment of the foulant molecules in the bulk solution to the fouling layer. That is, fouling at this stage is governed by foulant–foulant interactions. Presented below are such measurements for our NOM and NF membrane system under solution chemical

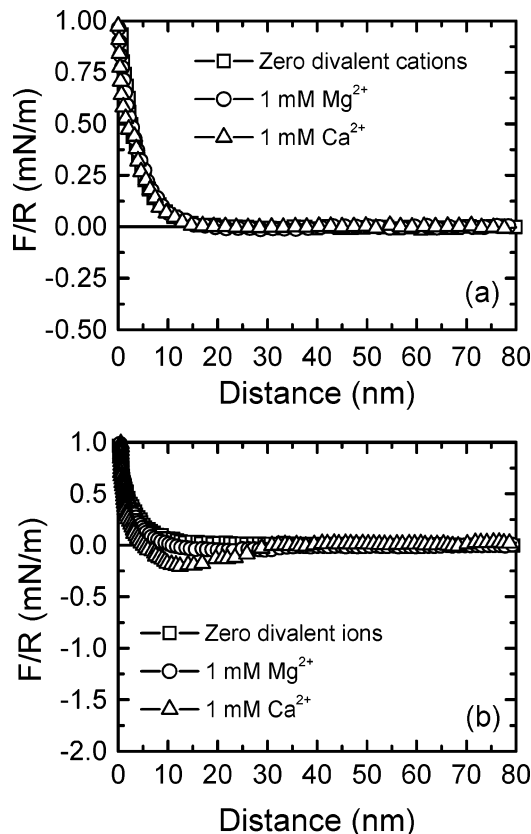


FIGURE 6. Interaction forces between the CML colloid probe and the clean membrane surface as a function of separation distance under various solution chemistries: (a) extending (approaching) force curves and (b) retracting force curves. The test solution contained 1 mM NaHCO₃, divalent cations as indicated, and NaCl to adjust the total ionic strength to 10 mM. The solution pH during the measurements was fixed at 8.1.

compositions similar to those employed in the fouling experiments.

(a) Foulant–Membrane Interactions. The force measurements were first conducted in humic acid free solutions, where the interfacial forces between the CML colloid probe (surrogate for humic acid) and the clean (foulant-free) membrane surface were measured. These forces represent the interaction forces between a humic acid molecule in the bulk solution and the clean membrane surface, which control the initial attachment of humic acid molecules to the membrane surface. The solution chemistries tested were identical to those used in the fouling experiments described above. Both the extending (approaching) and retracting parts of the force curves were analyzed, and the corresponding force versus distance profiles are presented in Figure 6. When divalent cations were absent, the force data obtained at a total ionic strength of 10 or 100 mM were similar. Therefore, only the data obtained at a total ionic strength of 10 mM are presented here.

Figure 6a displays the forces that the CML colloid probe experiences when approaching the clean membrane surface. This approaching part of the force curve simulates the process where the organic foulant is brought to the membrane surface by the convective permeate flow. Essentially, identical approaching force curves were obtained in all the three electrolyte solutions, indicating Mg²⁺ or Ca²⁺ had roughly the same double layer compressing effect as Na⁺ at the same total ionic strength. The CML particle experienced noticeable electrostatic double layer repulsion within 20 nm from the membrane surface and this repulsive force increased mark-

edly at smaller separations until the particle came into contact with the membrane surface at near zero separation distance.

Contrary to the approaching curves, the CML particle experienced different levels of adhesion forces when it was retracted away from the membrane surface after being brought into contact with the membrane surface. As shown in Figure 6b, the CML particle did not experience any adhesion force (i.e., negative values of F/R) when the solution was composed of only monovalent ions. When 1 mM Mg^{2+} was present in solution, there was very slight adhesion, that is, 0.06 ± 0.01 mN/m (indicated by the maximum negative value of F/R). The adhesion force increased significantly up to 0.21 ± 0.04 mN/m when the solution contained 1 mM Ca^{2+} , indicating that Ca^{2+} ions induced a stronger interaction between the carboxylic (COO^-) groups of the CML particle and the functional groups on the membrane surface. For our piperazine based aromatic NF membrane, the predominant functional groups at pH 8.1 are carboxylic, as indicated by the measured negative zeta potential.

The forces measured during the approach and retraction of the colloid probe determine the tendency of the CML particle (and presumably humic acid foulant) to attach to the membrane surface and the strength of the attachment, respectively. Therefore, the combination of the two measurements is related to the initial fouling rate of the membrane, provided the hydrodynamic conditions in the membrane system remain constant. Consequently, the difference in the adhesion forces shown in Figure 6b suggests that the effect of ionic composition on the initial fouling rate of the NF-270 membrane should follow the order of $Ca^{2+} > Mg^{2+} > Na^+$. However, this initial stage of fouling is very rapid as monolayer coverage on the membrane can be attained in a very short period of time. Thus, for most practical applications, the rate and extent of fouling are determined by the interaction between bulk foulant molecules and foulant molecules deposited in the fouling layer.

(b) Foulant–Foulant Interaction. The interaction forces between the CML particle (representing foulant molecules in the bulk solution) and foulants on the membrane surface (i.e., in the fouling layer) were also measured. Because of the difficulty in using a fouled membrane sample in the AFM liquid cell without disturbing the foulant layer, Suwannee River humic acid (SRHA) solution was injected into the fluid cell and equilibrated for 30 min so that a layer of SRHA molecules could adsorb on the clean membrane surface to simulate the foulant layer. It is likely that humic molecules also adsorbed to the CML particle in the liquid cell. The interaction between the CML particle and the membrane surface with the adsorbed humic layer then represents the foulant–foulant interaction. The ionic compositions of the SRHA solutions were identical to those used in the bench-scale fouling experiments.

The extending (approaching) and retracting parts of the force curves are presented in Figure 7, panels a and b, respectively. As shown in Figure 7a, the effect of Mg^{2+} on the approaching part of the force curve was similar to that of Na^+ . Electrostatic double layer repulsion existed within approximately 20 nm from the membrane surface, similar to our earlier observation with humic-free solution. However, a significant attractive force was observed when Ca^{2+} ions were present in solution. The CML particle first encountered a slight repulsion at a distance of about 25 nm. Then, at 21 nm, the net force became attractive and reached 0.23 ± 0.02 mN/m at 17 nm. These results indicate a strong attractive interaction between the CML particle and the humic acid molecules on the membrane surface, induced by chemical interaction with Ca^{2+} ions as discussed later in this paper.

When the colloid probe was retracted (Figure 7b), the results indicate that the Ca^{2+} ions caused a substantial adhesion of the CML to the fouled membrane surface (1.57

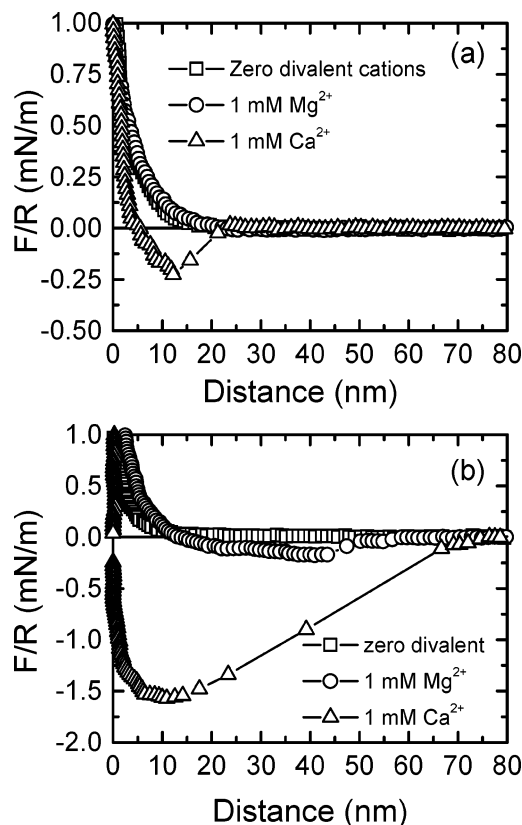


FIGURE 7. Interaction forces between the CML colloid probe and the fouled membrane surface as a function of separation distance under various solution chemistries: (a) extending (approaching) force curves and (b) retracting force curves. The test solution contained 20 mg/L SRHA, 1 mM $NaHCO_3$, divalent cations as indicated, and NaCl to adjust the total ionic strength to 10 mM. The solution pH during the measurements was fixed at 8.1.

± 0.12 mN/m). Although adhesion was also observed in the presence of Mg^{2+} , the magnitude of the adhesion force, 0.18 ± 0.02 mN/m, was much lower. No adhesion was observed when divalent cations were not present.

The interfacial force measurements with and without SRHA showed that the ionic solution composition had a similar effect on foulant–membrane and foulant–foulant interactions, with the magnitude of the adhesion forces following the order of $Ca^{2+} > Mg^{2+} > Na^+$. This result is in agreement with the membrane fouling behavior observed under similar solution chemistries in the bench-scale fouling experiments, with the rate of flux decline following the order of $Ca^{2+} > Mg^{2+} > Na^+$ (Figure 5). The attractive force upon approach to the membrane surface and the strong adhesion caused by Ca^{2+} , and likewise the much faster membrane flux decline with Ca^{2+} , point to a mechanism other than charge screening or neutralization, as we discuss later in this paper.

Chemical Cleaning and Flux Recovery. Chemical cleaning of the fouled membrane was conducted using deionized water, NaOH, EDTA, and SDS following the procedure described in Materials and Methods. As shown in the previous section, membrane flux decline was fairly small in the absence of Ca^{2+} ions in solution. Fouling experiments under these conditions were stopped after filtering 1.6 L feed solution through the membrane, which took more than 300 min. After the membrane was cleaned, a foulant-free electrolyte solution, with identical ionic composition to the feed foulant solution, was filtered through the membrane to measure the recovered flux. Membrane samples fouled with SRHA under these conditions (i.e., with Na^+ or Mg^{2+}) could be easily cleaned by all the chemical cleaning solutions tested, and

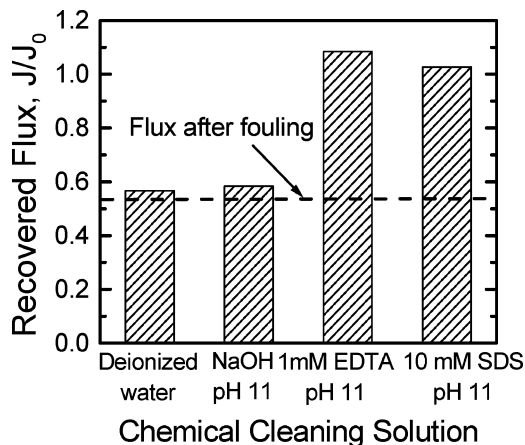


FIGURE 8. Recovered permeate water flux after cleaning with different cleaning chemicals. The feed solution contained 1 mM NaHCO_3 , 1 mM CaCl_2 , and NaCl to adjust the total ionic strength to 10 mM. Other experimental conditions: pH = 8.1 and the applied pressure was the same as that used in the preceding fouling runs.

the flux was completely recovered after deionized water cleaning alone. For experiments with feed solutions containing Ca^{2+} , the fouling runs were stopped when the permeate flux decreased to approximately 50% of the initial flux. The chemical cleaning results presented below are all for membrane samples fouled with feed solutions containing Ca^{2+} .

(a) Chemical Cleaning Efficiency. Figure 8 compares the recovered permeate flux of membrane samples fouled in the presence of Ca^{2+} after cleaning with the four chemical cleaning agents. The EDTA concentration used was 1 mM while the SDS concentration was 10 mM. Chemical cleaning was conducted at pH 11, except for the deionized water. In contrast to observations when the membrane was fouled in the presence of Na^+ or Mg^{2+} , deionized water and NaOH solution were both ineffective in recovering the permeate water flux after the membrane was fouled by feed solutions containing Ca^{2+} ions. The recovered fluxes were only 5 and 7% higher than the final flux after fouling for deionized water and NaOH cleaning, respectively. The poor efficiency of caustic cleaning suggests that the severe fouling in the presence of Ca^{2+} cations was not merely caused by conformational changes of SRHA due to electrostatic interactions (9).

EDTA and SDS cleaning, on the other hand, recovered the initial clean membrane water flux, indicating complete removal of SRHA from the membrane surface. A visual inspection of the membrane after cleaning also revealed no visible SRHA remaining. The recovered flux after EDTA or SDS cleaning was slightly higher than the original clean membrane flux, probably because of a very small amount of SRHA and EDTA or SDS remaining on the membrane surface, which made the membrane slightly more hydrophilic (3).

(b) Effect of Cleaning Solution pH. Chemical cleaning with EDTA or SDS was also conducted at ambient (unadjusted) pH to determine the effect of solution pH on chemical cleaning efficiency. The recovered permeate fluxes are presented in Figures 9 and 10 for EDTA and SDS cleaning, respectively. Results clearly show that cleaning efficiency of EDTA strongly depends on solution pH. At ambient pH (4.8 for the 1 mM EDTA solution), the recovered flux after EDTA cleaning was 35% lower than cleaning with EDTA at pH 11. The reason for this marked difference in cleaning efficiency will be explained later when we propose the cleaning mechanisms of fouled membranes. On the other hand, solution pH showed very little effect on SDS cleaning.

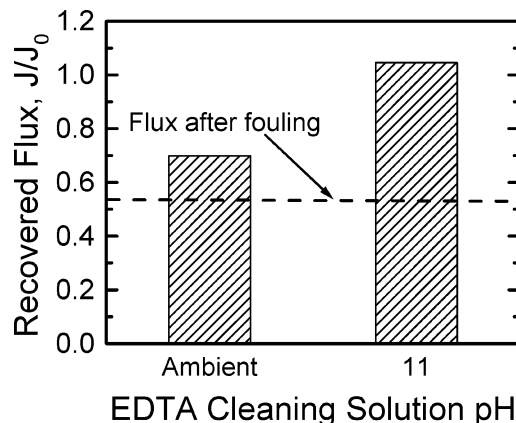


FIGURE 9. Recovered permeate water flux after cleaning with EDTA solutions of different pH. The EDTA concentration of the cleaning solutions was 1 mM. The feed solution contained 1 mM NaHCO_3 , 1 mM CaCl_2 , and NaCl to adjust the total ionic strength to 10 mM. Other experimental conditions: pH = 8.1 and the applied pressure was the same as that used in the preceding fouling runs.

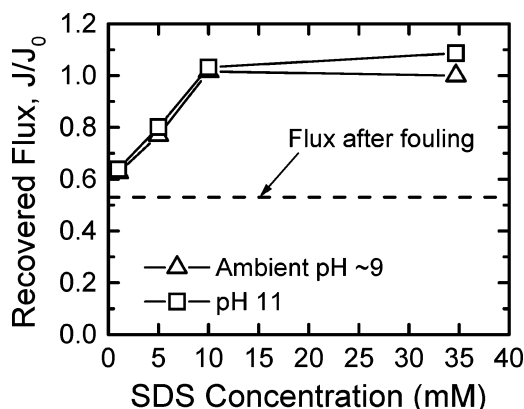


FIGURE 10. Effect of SDS concentration and cleaning solution pH on permeate water flux recovery. The feed solution contained 1 mM NaHCO_3 , 1 mM CaCl_2 , and NaCl to adjust the total ionic strength to 10 mM. Other experimental conditions: pH = 8.1 and the applied pressure was the same as that used in the preceding fouling runs.

However, the ambient pH of the SDS solution (approximately 9) was much higher than that of the EDTA solution (pH 4.8). The difference between the ambient pH and pH 11 might not be large enough to cause significant difference in chemical cleaning efficiency.

(c) Effect of SDS Concentration. SDS cleaning was performed using various SDS concentrations at both ambient pH (pH 9) and pH 11. Figure 10 shows how the recovered flux increased with increasing SDS concentration. Similar effect of cleaning chemical (mixture of EDTA, SDS, and NaOH) concentration on flux recovery of a reverse osmosis membrane was reported by Madaeni et al. (22). Very little flux recovery—11 and 12% of the initial flux for ambient pH and pH 11, respectively—was achieved by cleaning with 1 mM SDS. This is in agreement with the results by Lee et al. (59), reporting poor cleaning efficiency by SDS at this concentration when an ultrafiltration membrane was fouled by surface or groundwater NOM. For both solution pH values tested, the recovered flux increased with increasing SDS concentration. At 10 mM SDS concentration or higher, cleaning completely recovered the initial clean membrane water flux. This critical concentration (i.e., 10 mM SDS) is very close to the critical micelle concentration (CMC) of SDS, reported as 8.36 mM in deionized water at 20 °C (60). The results suggest that formation of micelles may be critical for SDS cleaning of NOM-fouled membranes. The possible

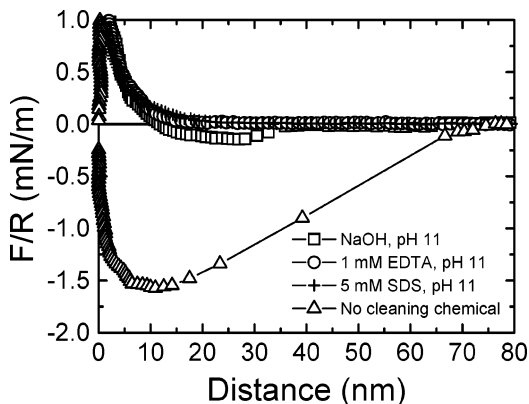


FIGURE 11. Interaction forces between the CML colloid probe and the SRHA fouled membrane surface in the presence of various chemical cleaning agents. The test solution contained 20 mg/L SRHA, cleaning chemicals as indicated, 1 mM NaHCO_3 , 1 mM CaCl_2 , and NaCl to adjust the total ionic strength to 10 mM. The solution pH during the measurements was fixed at 8.1.

mechanisms involved in surfactant cleaning of NOM fouled membranes are described in detail later in this paper.

Effect of Chemical Cleaning on NOM Adhesion to the Membrane Surface. During chemical cleaning, the foulant molecules in the fouling layer experience two types of forces: an adhesion force that keeps them on the surface and a hydrodynamic shearing force removing them to the bulk phase. Therefore, the strength of the adhesion force among foulant molecules in the fouling layer determines the ease of membrane cleaning for given hydrodynamic conditions.

Interfacial force measurements using the CML colloid probe were performed in the presence of the chemical cleaning agents to investigate the effect of chemical cleaning on foulant–foulant interactions in the fouling layer. Since significant fouling was only observed in the presence of Ca^{2+} , the test solutions contained 1 mM CaCl_2 . Other conditions were similar to those used in the foulant–foulant interaction force measurements described previously, namely, total ionic strength of 10 mM and 20 mg/L SRHA. In each test solution, one of the following cleaning chemicals was added: NaOH, 1 mM EDTA, or 5 mM SDS. The solution pH was adjusted to 11 in all runs. These solution conditions simulate the solution chemistry during the bench-scale chemical cleaning experiments described earlier.

Figure 11 compares the adhesion forces measured with and without the addition of a chemical cleaning agent. As shown, addition of cleaning chemicals dramatically reduces the adhesion force between the CML particle and the fouled membrane surface. It is striking that EDTA and SDS at the tested concentrations eliminated the adhesion force completely. However, a significant adhesion force, 0.14 ± 0.01 mN/m, still existed in the presence of NaOH at pH 11. The relative magnitudes of the adhesion forces are inversely related to the relative chemical cleaning efficiencies obtained using the same cleaning agents. That is, the elimination of the adhesion force in the presence of EDTA or SDS corresponds to complete flux recovery, whereas the remaining adhesion force with NaOH addition corresponds to the poor cleaning efficiency of NaOH.

Although the adhesion force was reduced significantly by NaOH compared to without cleaning chemical addition, cleaning by NaOH was not efficient presumably because the hydraulic shearing force provided during cleaning was not high enough to overcome the remaining adhesion force. Also, the effect of SDS concentration on chemical cleaning was not reflected by the adhesion force data; the 5 mM SDS reduced the adhesion to zero, but it was not sufficient to

completely recover the membrane flux in the bench-scale fouling/chemical cleaning experiments (Figure 10). We attribute this result to the different ratios of the cleaning chemical concentration relative to the organic foulant mass in the AFM fluid cell and the stirred cell filtration system. In the stirred cell filtration unit, the foulant layer formed by accumulation of SRHA during filtration of approximately 1 L of 20 mg/L SRHA solution. That is, the total amount of humic acid on the fouled membrane in the stirred cell during chemical cleaning was much higher than that in the AFM fluid cell, which contained less than 1 mL of the 20 mg/L SRHA solution. Therefore, complete removal of the adhesion force in the AFM fluid cell could be attained at a lower concentration of SDS than in the bench-scale chemical cleaning experiments.

Mechanistic Models of NOM Fouling and Chemical Cleaning. On the basis of the experimental data presented above with both the bench-scale fouling/cleaning experiments and the AFM interaction force measurements, mechanisms of humic acid fouling and chemical cleaning of NF membrane are proposed.

(a) Enhanced Fouling by Divalent Cations. When monovalent cations are present, the fouling process is determined by electrostatic and hydrophobic interactions between the foulant and the clean membrane surface at the initial stage and between the foulant molecules in the bulk solution and foulants on the fouling layer surface once the membrane is covered with the foulants. Because of the negative surface charge of the NF-270 membrane, a net repulsive electrostatic force exists between the humic acid molecules (represented by the CML particle) and the membrane as observed in Figure 6a. A similar net repulsive force exists when the membrane surface is covered by a layer of humic acid molecules (Figure 7a) because of the negative charge of SRHA molecules. As a result of the strong electrostatic repulsion, there is no adhesion between the CML particle or humic acid molecules and the clean or fouled membrane surfaces when only monovalent ions are present as indicated in Figures 6b and 7b. Consequently, the accumulation of humic acid on the membrane surface is very slow and the foulant layer formed is thin and loose, leading to a very low fouling rate, as shown in Figure 4.

Compared to monovalent cations, divalent cations can screen charges more effectively and therefore have a greater effect on reducing double repulsion. However, force measurements in Figure 6a show no difference in electrostatic repulsion with and without divalent cations at a fixed total ionic strength. Apparently, the changes in membrane surface potential and foulant surface charge by divalent cations are too small to cause measurable changes in electrostatic repulsion compared to the case with monovalent cations when the same total ionic strength of 10 mM was used. This is consistent with the similar fouling rate and foulant–membrane interaction forces measured with monovalent ions at total ionic strengths of 10 and 100 mM. For the same reason, the adhesion force between humic acid molecules and the clean membrane surface is negligible in the presence of Mg^{2+} as demonstrated in Figure 6b.

In addition to effective charge screening, divalent cations (Ca^{2+} and Mg^{2+}) form metal–humic complexes (61) and therefore effectively reduce the negative charge of humic acid (62). Moreover, as a result of the reduced interchain electrostatic repulsion due to neutralization of negative charges of functional groups, humic acid molecules form a small, coiled conformation (63), and subsequently a more compact fouling layer (3). The increased adhesion in the presence of Mg^{2+} (Figure 7b) is an indication for these changes. Because of the higher adhesion force and the more compact structure of humic acid, Mg^{2+} causes higher fouling rate than Na^+ , as shown in Figure 5.

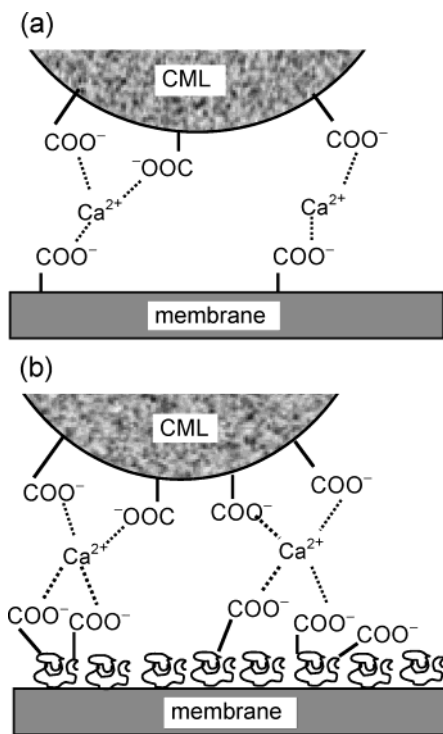


FIGURE 12. Schematic illustration of the influence of Ca^{2+} on the interaction between the CML particle and (a) the clean membrane surface and (b) the fouled membrane surface. The binding sites shown are solely for illustration purposes.

Unlike Mg^{2+} , Ca^{2+} caused significant adhesion of the CML colloid probe to the clean membrane surface (Figure 6b). This may be attributed to intermolecular bridging by Ca^{2+} (17), which associates the COO^- functional groups on the CML particle, representing humic acid molecules in the bulk solution, with a small number of COO^- groups on the clean membrane surface. A schematic illustration of this proposed mechanism is presented in Figure 12a.

Once the membrane is fouled, the membrane surface is covered by a layer of humic acid molecules, rendering it a greater number of COO^- functional groups. These COO^- groups associate with those on the CML colloid probe via Ca^{2+} bridging. The overall Ca^{2+} binding force between the CML particle and the humic acid molecules on the membrane

surface becomes much stronger than the electrostatic repulsion, resulting in a net attractive force when the CML particle approaches the fouled membrane surface. Because of the much greater number of COO^- groups on the fouled membrane surface, the adhesion force also increases greatly compared to when clean membrane surface was used. The complexation/bridging effect of Ca^{2+} with the fouled membrane is schematically depicted in Figure 12b.

During membrane filtration, Ca^{2+} forms intramolecular complexes with humic acid (predominantly with carboxylic groups), rendering the humic acid molecules a small, coiled conformation. At the same time, intermolecular bridging formed by Ca^{2+} between carboxylic groups arranges the humic acid molecules into a "cross-linked" structure in the fouling layer, with each humic acid molecule strongly associated with humic acid molecules around it. As a result, the fouling layer formed in the presence of Ca^{2+} is very compact and highly resistant to hydrodynamic forces. An illustration of the structure of the humic acid fouling layer formed in the presence of Ca^{2+} on the basis of our proposed mechanism is shown in Figure 13a.

(b) Mechanisms of Chemical Cleaning with EDTA. As described above, humic acid fouling in the presence of Na^+ or Mg^{2+} is mainly controlled by electrostatic interactions. Therefore, cleaning with a low ionic strength solution, such as deionized water, is able to achieve efficient flux recovery. Our discussion will therefore focus on cleaning mechanisms when Ca^{2+} ions are present in the feedwater.

In the presence of Ca^{2+} ions, the humic acid molecules in the fouling layer are bound to each other by Ca^{2+} . Since EDTA forms a stronger complex with Ca^{2+} , humic acid molecules originally associated with Ca^{2+} ions are replaced by EDTA via a ligand exchange reaction. The intermolecular bridges among humic acid molecules as well as those between humic acid molecules and the membrane surface are then destructed, as indicated by the zero adhesion force with EDTA shown in Figure 11. Thus, the foulant layer loses its cross-linked, gel-like structure. At the same time, interchain repulsion is resumed and humic acid molecules return to the original loose conformation due to the destruction of intramolecular Ca^{2+} -humic complexes. These detached individual humic acid molecules can then be easily rinsed off the membrane surface. The changes in the fouling layer structure and humic acid conformation as a result of EDTA cleaning are depicted schematically in Figure 13.

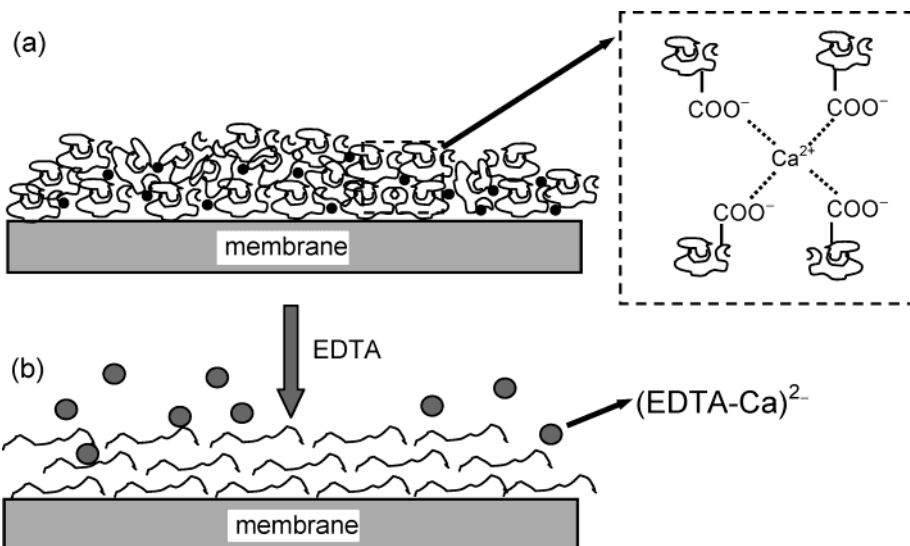


FIGURE 13. Schematic illustration of the change in the organic fouling layer structure by EDTA. (a) Compact fouling layer formed in the presence of Ca^{2+} . (b) Loose structure of the fouling layer after EDTA addition. The binding sites shown are solely for illustration purposes.

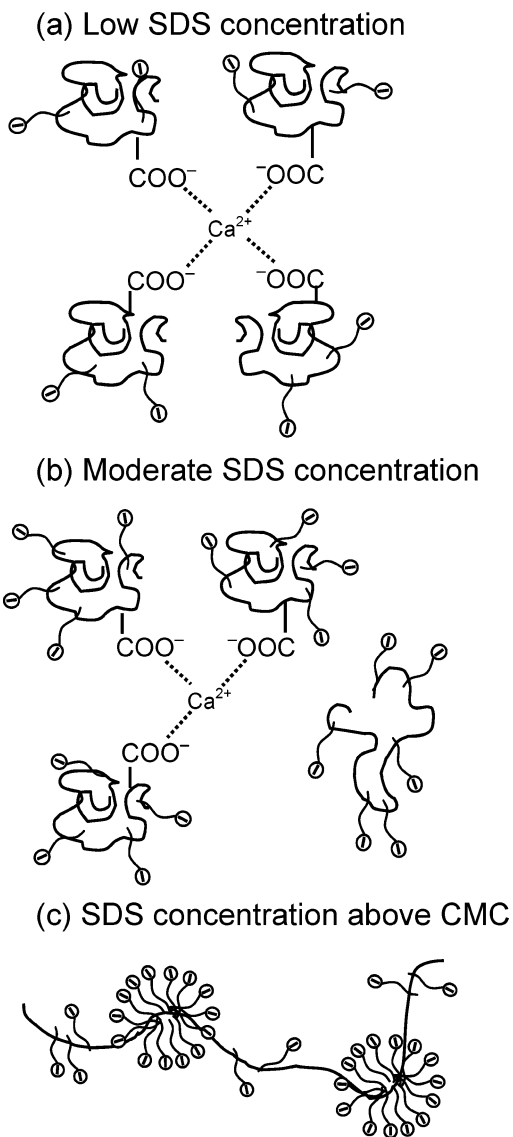


FIGURE 14. Mechanism of humic acid solubilization by SDS: (a) low SDS concentration, (b) moderate SDS concentration, and (c) SDS concentration exceeding the CMC. The binding sites shown are solely for illustration purposes.

The cleaning efficiency of EDTA strongly depends on solution pH because the number of deprotonated carboxylic groups of EDTA is a function of pH. The pK_a values of EDTA are 2.72, 3.24, 6.68, and 11.12 (62). At the ambient pH of 1 mM EDTA solution (pH 4.8), only two of the four carboxylic groups are deprotonated, while at pH 11 almost all the carboxylic groups are deprotonated and available for Ca^{2+} complexation.

(c) Mechanisms of Chemical Cleaning with SDS. Surfactants, such as SDS, are known to solubilize macromolecules by forming micelles around them (64). The proposed mechanism of SDS cleaning is depicted in Figure 14. Because of the amphiphilic character of SDS, the hydrophobic tails of SDS molecules adsorb onto humic acid molecules. The adsorbed SDS molecules reduce the hydrophobicity of humic acid and help relaxing the coiled structure. At a low SDS concentration, for instance 1 mM, the hydrophilic interaction rendered by the adsorbed SDS is not strong enough to break the intermolecular bridging formed with Ca^{2+} (Figure 14a). Therefore, very little flux recovery was achieved after cleaning (Figure 10). When a higher SDS concentration is used (Figure 14b), more SDS molecules partition into the foulant layer

and the increased hydrophilic interaction results in breakup of some Ca^{2+} bindings. Some humic acid molecules are then solubilized into the aqueous phase and are flushed away by the hydrodynamic shearing force. Once the SDS concentration exceeds the CMC (8.36 mM in deionized water), micelles form in the cleaning solution (Figure 14c). These micelles diffuse into the fouling layer, where they dissociate and adsorb as monomers on humic acid molecules (65, 66). Local SDS micelles may also form at hydrophobic portions of humic acid molecules (67). The resulting solubilization force is then strong enough to break up all the Ca^{2+} induced bridges (as indicated by the zero adhesion with SDS shown in Figure 11), leading to release of the humic acid to the aqueous phase. The local micelles formed also help keeping the humic acid molecules from reprecipitating.

Acknowledgments

Funding was provided by the U.S. Bureau of Reclamation under the Desalination and Water Purification Research and Development Program (DWPR).

Literature Cited

- (1) Livingston, A.; Peeva, L.; Han, S. J.; Nair, D.; Luthra, S. S.; White, L. S.; Dos Santos, L. M. F. In *Advanced Membrane Technology*; Li, N. N., et al., Eds.; New York Academy of Sciences: New York, 2003; Vol. 984, pp 123–141.
- (2) Marcucci, M.; Ciabatti, I.; Matteucci, A.; Vernaglione, G. In *Advanced Membrane Technology*; Li, N. N., et al., Eds.; New York Academy of Sciences: New York, 2003; Vol. 984, pp 53–64.
- (3) Hong, S.; Elimelech, M. *J. Membr. Sci.* **1997**, *132*, 159–181.
- (4) Childress, A. E.; Elimelech, M. *Environ. Sci. Technol.* **2000**, *34*, 3710–3716.
- (5) Seidel, A.; Elimelech, M. *J. Membr. Sci.* **2002**, *203*, 245–255.
- (6) Ghosh, K.; Schnitzer, M. *Soil Sci.* **1980**, *129*, 266–276.
- (7) Braghetta, A. Doctoral Dissertation, University of North Carolina, Chapel Hill, NC, 1995.
- (8) Jucker, C.; Clark, M. M. *J. Membr. Sci.* **1994**, *97*, 35–52.
- (9) Braghetta, A. H.; DiGiano, F. A.; Ball, W. P. *J. Environ. Eng., ASCE* **1997**, *123*, 628–641.
- (10) Yuan, W.; Zydny, A. L. *Desalination* **1999**, *122*, 63–76.
- (11) Yuan, W.; Zydny, A. L. *Environ. Sci. Technol.* **2000**, *34*, 5043–5050.
- (12) Jones, K. L.; O'Melia, C. R. *J. Membr. Sci.* **2000**, *165*, 31–46.
- (13) Braghetta, A.; DiGiano, F. A.; Ball, W. P. *J. Environ. Eng., ASCE* **1998**, *124*, 1087–1098.
- (14) Kabsch-Korbutowicz, M.; Majewska-Nowak, K.; Winnicki, T. *Desalination* **1999**, *126*, 179–185.
- (15) Cho, J.; Amy, G.; Pellegrino, J. *J. Membr. Sci.* **2000**, *164*, 89–110.
- (16) Schäfer, A.; Fane, A. G.; Waite, T. D. *Desalination* **1998**, *118*, 109–122.
- (17) Yoon, S.; Lee, C.; Kim, K.; Fane, A. G. *Water Res.* **1998**, *32*, 2180–2186.
- (18) Walton, N. R. G. *Desalination* **1988**, *68*, 29–33.
- (19) Ebrahim, S. *Desalination* **1994**, *96*, 225–238.
- (20) Sathwani, J. J.; Veza, J. M. *Desalination* **2001**, *139*, 177–182.
- (21) Mohammadi, T.; Madaeni, S. S.; Moghadam, M. K. *Desalination* **2003**, *153*, 155–160.
- (22) Madaeni, S. S.; Mohamamdi, T.; Moghadam, M. K. *Desalination* **2001**, *134*, 77–82.
- (23) Liikanen, R.; Yli-Kuivila, J.; Laukkanen, R. *J. Membr. Sci.* **2002**, *195*, 265–276.
- (24) Ren, D. Q. *Desalination* **1987**, *62*, 363–371.
- (25) Osta, T. K.; Bakheet, L. M. *Desalination* **1987**, *63*, 71–80.
- (26) Trägårdh, G. *Desalination* **1989**, *71*, 325–335.
- (27) Weis, A.; Bird, M. R.; Nystrom, M. *J. Membr. Sci.* **2003**, *216*, 67–79.
- (28) Bird, M. R.; Fryer, P. J. *Trans. Inst. Chem. Eng., Part C* **1991**, *69*, 13–21.
- (29) Tuladhur, T. R. Doctoral Dissertation, University of Cambridge, 2001.
- (30) Graham, S. I.; Reitz, R. L.; Hickman, C. E. *Desalination* **1989**, *74*, 113–124.
- (31) Ebrahim, S.; Malik, A. *Desalination* **1987**, *66*, 201–221.
- (32) Farinas, M.; Granda, J. M.; Gurtubai, L.; Villagra, M. J. *Desalination* **1987**, *66*, 385–402.
- (33) Lindau, J.; Jonsson, A. S. *J. Membr. Sci.* **1994**, *87*, 71–78.
- (34) Daufin, G.; Merin, U.; Labbe, J. P.; Quemerais, A.; Kerherve, F. L. *Biotechnol. Bioeng.* **1991**, *38*, 82–89.

- (35) Bohner, H. F.; Bradley, R. L. *J. Dairy Sci.* **1992**, *75*, 718–724.
- (36) Butt, H. J. *Biophys. J.* **1991**, *60*, 1438–1444.
- (37) Ducker, W. A.; Senden, T. J.; Pashley, R. M. *Langmuir* **1992**, *8*, 1831–1836.
- (38) Weisenhorn, A. L.; Maivald, P.; Butt, H. J.; Hansma, P. K. *Phys. Rev. B* **1992**, *45*, 11226–11232.
- (39) Butt, H. J. *Biophys. J.* **1992**, *63*, 578–582.
- (40) Rutland, M. W.; Senden, T. J. *Langmuir* **1993**, *9*, 412–418.
- (41) Radmacher, M.; Fritz, M.; Cleveland, J. P.; Walters, D. A.; Hansma, P. K. *Langmuir* **1994**, *10*, 3809–3814.
- (42) Milling, A.; Mulvaney, P.; Larson, I. *J. Colloid Interface Sci.* **1996**, *180*, 460–465.
- (43) Mizes, H. A.; Loh, K. G.; Miller, R. J. D.; Ahuja, S. K.; Grabowski, E. F. *Appl. Phys. Lett.* **1991**, *59*, 2901–2903.
- (44) Biggs, S. *Langmuir* **1995**, *11*, 156–162.
- (45) Milling, A.; Biggs, S. *J. Colloid Interface Sci.* **1995**, *170*, 604–606.
- (46) Cleveland, J. P.; Schaffer, T. E.; Hansma, P. K. *Phys. Rev. B* **1995**, *52*, 8692–8695.
- (47) Meagher, L. C.; Savill, J. S.; Baker, A.; Fuller, R. W.; Haslett, C. *J. Leukocyte Biol.* **1992**, *52*, 269–273.
- (48) Tsao, Y. H.; Yang, S. X.; Evans, D. F.; Wennerstrom, H. *Langmuir* **1991**, *7*, 3154–3159.
- (49) Considine, R. F.; Hayes, R. A.; Horn, R. G. *Langmuir* **1999**, *15*, 1657–1659.
- (50) Bowen, W. R.; Hilal, N.; Lovitt, R. W.; Sharif, A. O.; Williams, P. M. *J. Membr. Sci.* **1997**, *126*, 77–89.
- (51) Bowen, W. R.; Hilal, N.; Jain, M.; Lovitt, R. W.; Sharif, A. O.; Wright, C. J. *Chem. Eng. Sci.* **1999**, *54*, 369–375.
- (52) Hilal, N.; Bowen, W. R. *Desalination* **2002**, *150*, 289–295.
- (53) Hilal, N.; Bowen, W. R.; Lovitt, R. W.; Wright, C. J. *Eng. Life Sci.* **2002**, *2*, 131–135.
- (54) Hilal, N.; Mohammad, A. W.; Atkin, B.; Darwish, N. A. *Desalination* **2003**, *157*, 137–144.
- (55) Freger, V.; Gilron, J.; Belfer, S. *J. Membr. Sci.* **2002**, *209*, 283–292.
- (56) Childress, A. E.; Elimelech, M. *J. Membr. Sci.* **1996**, *119*, 253–268.
- (57) Elimelech, M.; Chen, W. H.; Waypa, J. J. *Desalination* **1994**, *95*, 269–286.
- (58) Israelachvili, J. N. *Intermolecular and Surface Forces*, 2nd ed.; Academic Press: New York, 1992.
- (59) Lee, H.; Amy, G.; Cho, J. W.; Yoon, Y. M.; Moon, S. H.; Kim, I. S. *Water Res.* **2001**, *35*, 3301–3308.
- (60) Mukerjee, P.; Mysels, K. J. *NSRDS–NBS 36*; U.S. Department of Commerce, National Bureau of Standards: Washington, DC, 1970.
- (61) Schnitzer, M.; Khan, S. U. *Humic Substances in the Environment*; Marcel Dekker: New York, 1972.
- (62) Morel, F. M. M.; Hering, J. G. *Principles and Applications of Aquatic Chemistry*; Wiley-Interscience: New York, 1993.
- (63) Clark, M. M.; Lucas, P. J. *J. Membr. Sci.* **1998**, *143*, 13–25.
- (64) Rosen, M. J. *Surfactant and Interfacial Phenomena*, 2nd ed.; Wiley: New York, 1989.
- (65) Carroll, B. J. *J. Colloid Interface Sci.* **1981**, *79*, 126–135.
- (66) Carroll, B. J.; Orourke, B. G. C.; Ward, A. J. I. *J. Pharm. Pharmacol.* **1982**, *34*, 287–292.
- (67) Deo, N.; Somasundaran, P. *Langmuir* **2003**, *19*, 2007–2012.

Received for review December 17, 2003. Revised manuscript received June 8, 2004. Accepted June 18, 2004.

ES0354162